EARTH OBSERVATION AND GEOMATICS ENGINEERING
website: https://eoge.ut.ac.ir

Long-term evaluation of temperature profiles derived from space-based GPS meteorology with radiosonde measurements over Iran

Ali Sam Khaniani *

Babol Noshirvani University of Technology, Civil Engineering Department, P.O. Box484, Shariati Ave, Babol, Mazandaran 47148-71167, Iran

Article history:

Received: 25 December 2019, Received in revised form: 1 April 2020, Accepted: 5 April 2020

ABSTRACT

In recent years, space-based GPS Radio occultation (RO) data have been recognized as a valuable resource in the advancement of various fields such as meteorology, numerical weather forecasting, climate studies, and ionospheric research. Although the atmospheric temperature profiles derived from this space-based technique have been used in a few national studies, long-term evaluation of these data and their widespread use has not been performed, especially by Iranian meteorologists. In this paper, RO temperature profiles obtained from COSMIC, SACC, GRACE, TerraSAR-X, KOMPSAT5, METOP-A, and METOP-B satellite missions were compared with their corresponding radiosonde measurements in five different geographic regions of Iran. Based on the data collected from 2006 to 2018, statistical assessments were carried out at 4km height intervals between the altitudes 0–36 km. The RO temperature data that occur 300 km away and 2 hours from radiosonde measurements were selected for comparison. The results in all stations show that, compared to radiosonde, GPS RO is acceptable for measuring the atmospheric temperature over the study area. Agreement of space-based GPS RO derived temperature below 28 km with respective values obtained from radiosonde in terms of mean bias and standard deviation were 1. 0.24 K and 1.5 K, respectively. Overall, seasonal comparisons indicated that there is no significant relationship between the behavior of mean bias and seasonal changes.

KEYWORDS

GPS RO

Radiosonde

Temperature Profile

Bias

Long-term comparison

1. Introduction

Global weather and climate modeling requires proper monitoring of atmospheric parameters such as air temperature and humidity. In recent years, due to global warming resulted from climate change, the analysis of behavior and anomaly of these parameters have received much attention. Therefore, a deeper understanding of the changes and behavior of parameters, such as atmospheric temperature, has been taken into account with the help of the data of different elevation layers obtained by new methods (Sobrino et al., 2014; Chang et al., 2018). Furthermore, long-term, stable, high-accuracy temperature data are critical to understanding climate processes and changes in the troposphere and stratosphere (Seidel et al., 2011; Thorne et al., 2011).

Conventionally, atmospheric properties used to be described through limited parameters close to the Earth's surface, such as temperature and relative humidity measured at meteorological stations. Radiosondes play a vital role in collecting atmospheric data that have been in use since the 1930s. Today, there is a network of more than 800 radiosonde stations worldwide (Kuo et al., 2005). Atmospheric parameters, such as temperature, pressure, humidity, and wind, are measured at different altitudes using meteorological balloons, which are valuable resources in climate studies and weather forecasts.

Radiosondes are common instruments for detecting temperature changes in the troposphere and lower stratosphere. Radiosonde upper-air atmospheric data can be utilized in data assimilation to improve numerical models of

* Corresponding author

E-mail addresses: ali.sam@nit.ac.ir (A. Sam Khaniani)

DOI: 10.22059/eoge.2020.297702.1073

weather forecasting, evaluation, and validation of remote sensing data, and in the study of the vertical structure atmosphere (Zhang et al., 2007). However, these data have limitations including, high cost, poor temporal resolution, inhomogeneous spatial coverage, and the need for sensor calibration (Kuo et al., 2005). Radiosonde data are usually available inland and suffer from low spatial resolution (Divakarla et al., 2006; Bohlinger et al., 2014). The vertical structure of the atmosphere is determined using local data, such as Radiosonde balloon measurements at specific times. However, the quality of different radiosonde sensors varies at different altitudes (Luers, 1997).

On the other hand, it is more than two decades that the GPS RO technique, which uses Low Earth Orbit (LEO) satellites, such as CHAMP, SACC, GRACE, COSMIC and some others, has been recognized as a new method for atmospheric profiling (Reigber et al., 2005; UCAR, 2006). The basis of this method is the delay and bending of radio signals from GPS satellites when passed through the atmosphere to reach receivers onboard LEO satellites (Kursinski et al., 1997). In this method, the vertical profiles of temperature, pressure, water vapor in the neutral atmosphere, and electron density in the ionosphere are obtained by calculating the refractive index values using the inverse Abel transformation. Hence, GPS RO provides valuable information on the vertical structure of the ionosphere, stratosphere, and troposphere. Besides, this atmospheric remote sensing method has unique features, such as global coverage, high vertical resolution, high accuracy, applicability to any weather conditions, and no need for calibration (Reigber et al., 2005). It should be noted that RO profiles are unaffected by the presence of clouds and have the same quality throughout the day and night.

Many studies have reported that GPS RO data are a valuable source of climatic and meteorological studies (Healy et al. 2005; Aparicio & Deblonde 2008; Renine, 2010; Le Marshall et al., 2012). Due to the unique features of GPS RO, its products can be used to improve numerical weather prediction models, prepare accurate geopotential heights, determine atmospheric gravity waves energy, and study the anomalies of electron density in the ionosphere (Anthes et al., 2000; Tsuda & Hocke, 2004).

Various studies have been conducted to validate the temperature profiles of GPS RO techniques that have shown the high quality of these products (Ware et al., 1996; Rocken et al., 1997; Wickert et al., 2001; Rossiter, 2003; Hajj et al., 2004; Wickert et al., 2004; Zhang et al., 2007; Kishore et al., 2009; Ho et al., 2012,2017). Based on previous studies, the accuracy of GPS RO temperature profiles has been reported to be about 1 K in the lower troposphere up to 40 km (Ware et al., 1996; Rocken et al., 1997). The temperatures of mid- to high latitudes were estimated to be less than 1 K using the CHAMP and GPS/MET missions, and less than 0.5 K using the ECMWF model implemented close to the tropopause and at altitudes 12 to 20 km (Wickert et al., 2001).

Rossiter (2003) compared RO profiles with different types of radiosonde measurements and showed that the RO technique is able to recognize the performance of various types of radiosonde. Another study found an accuracy of ± 0.6 K for temperature profiles obtained from the CHAMP mission between 5 to 15 km (Hajj et al., 2004).

Zhang et al. (2007) compared the atmospheric profiles of the CHAMP mission with the corresponding values obtained from radiosonde measurements in Western Australia. They found that the difference between the values of RO and radiosonde temperatures was less than 1 K at altitudes less than 14 km and less than 3 K near the tropopause. Ho et al. (2012) estimated the accuracy of GPS RO temperatures and the precision of the temperature trend of about 0.1 K and 0.06 K/5years, respectively.

Also, comparing the retrieval of different centers and examining the differences in co-located profiles of different GPS RO missions have shown the stability of temperature profiles attained from the space-based GPS meteorology (Anthes et al., 2008; Foelsche et al., 2009; Ho et al., 2011). The atmospheric profiles obtained from GPS observations of LEO satellites using the RO approach are of particular importance in meteorological applications and have the potential to improve atmospheric analyses (Le Marshall et al., 2010). So far, several studies have been conducted by both ground-based and space-based GPS meteorology in the study area (e.g., Sharifi et al., 2013a,b; Sharifi et al., 2016; Khaniani & Ghahremani, 2019; Khaniani et al., 2020). However, beneficial GPS RO data are not well-known by Iranian meteorologists and the number of studies using this technique is limited. Therefore, it is important to understand and compare these data using conventional methods, i.e., radiosonde, in the study area. In this study, the GPS RO temperature profiles of several satellite missions in Iran from 2006 to 2018 have been compared with those of radiosonde measurements. To this end, the data from the COSMIC, SACC, GRACE, KOMPSAT5, METOP-A, and METOP-B satellites will be compared with observations from five radiosonde stations over the study period.

Section 2 introduces the datasets and the study area. Then, Section 3 presents the retrieval of atmospheric profiles using the GPS RO technique. The results of long-term comparison of temperature profiles derived from GPS RO and radiosonde measurements are given in section 4. In this part, the differences between these two datasets at different altitudes and seasons will be statistically assessed over the period of 13 years. finally, the conclusions are drawn in the final section.

2. Data and study area

In this work, in order to measure the accuracy and stability of GPS RO temperature data in Iran, the observed temperature profiles at five radiosonde stations from 2006 to 2018 are used as reference values. The radiosonde used in this study is of the Visala RS92 type, and the observations were made at 00 and 12 UTC. Table 1 presents the geographical characteristics of the radiosonde stations used in this study. Also, Fig. 1 shows the spatial distribution of approximately homogeneous selected radiosonde stations. According to Fig. 1, for comparison purposes, the radiosonde observations in Tehran, Tabriz, Birjand, Kermanshah, and Shiraz Provinces are used. It should be noted that the climatic conditions of these areas are different. Therefore, the results of this statistical evaluation using the data of 13 years will have better reliability.

The RO technique initially used to determine the atmosphere of other planets such as Venus and Mars (Phinney & Anderson, 1968; Bird et al. 1992). Then, in 1996, the GPS / MET satellite mission was first launched to produce the Earth's atmosphere profiles using the RO techniques. Here, to study the accuracy of GPS RO temperature data, we have attempted to use the maximum number of profiles of LEO satellite missions. For this purpose, all available data of the 7 GPS RO missions listed in Table 2 were used. For each of the GPS RO missions, the number of profiles in latitudes 25-40 degrees North and longitudes 44-64 degrees East is given in Table 2. It also shows the time intervals during which the RO missions prepared data in the study area.

Table 1. Characteristics of the radiosonde stations used in this study.

Station Name	Longitude(°N)	Latitude(°E)	Height(m)
OIII	**35.6857**	**51.3036**	**1191.0**
OIMB	**32.8939**	**59.2903**	**1509.0**
OISS	**29.5392**	**52.5898**	**1484.0**
OICC	**34.3459**	**47.1581**	**1319.0**
OITT	**38.1305**	**46.2402**	**1359.0**

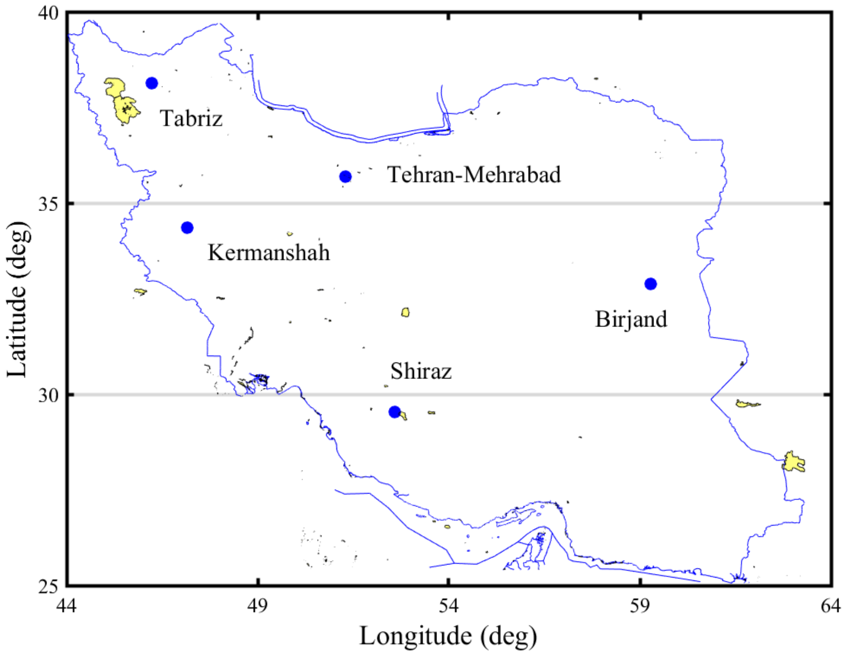

Figure 1. Spatial distribution of radiosonde stations in the study area.

For long-term comparison between RO and radiosonde temperatures, COSMIC data of 13 years, GRACE data of 11 years, SACC data of 6 years, TerraSAR-X data of 11 years, KOMPSAT-5 data of 4 years, METOPA data of 12 years, and METOP-B data of 6 years were collected from the University Corporation for Atmospheric Research (UCAR) website (http://www.cosmic.ucar.edu).

Among all datasets obtained in the region, the RO temperature profiles within a radius of 200 km from the radiosonde station position and less than 3 hours apart from the radiosonde observations were selected for statistical comparisons.

Table 2. Details of the GPS RO data used in this study from 2006 to 2018.

GPS RO missions	Data availability	Number of Profiles
COSMIC	2006-2018	43725
GRACE	2007-2017	2638
SACC	2006-2011	1858
TerraSAR-X	2008-2018	4131
KOMPSAT-5	2015-2018	2497
METOP-A	2007-2018	15994
METOP-B	2013-2018	8642

3. GPS RO temperature retrieval

About 30 GPS satellites are continuously transmitting signals in the L band frequency. Meanwhile, LEO satellites, which also have GPS receivers, rotate around the Earth in their orbit. At certain time intervals, GPS and LEO satellites are located on either side of the Earth and lose direct visibility between them, but due to the refraction gradient in the Earth's atmosphere, the GPS signal path bends and is received at LEO satellite. In such circumstances, the so-called Occultation occurs. Using GPS and LEO satellites ephemeride data via an inverse problem, the atmospheric profiles, such as temperature, pressure, and water vapor, can be retrieved (Hajj et al., 1994; Kursinski et al., 1996; Rocken et al., 1997). Fig. 2 demonstrates the geometry of a GPS RO measurement.

LEO satellites measure the phase and amplitude of signals transmitted by GPS satellites in the L band, as a function of time. The relative motion of LEO satellites with respect to GPS satellites as well as the presence of the atmosphere cause a Doppler shift of frequencies in GPS signals received in LEO satellites. The doppler shift values are obtained by time derivation of phase measurements, and along with accurate information about the position and velocity vector of both GPS and LEO satellites, they result in the estimation of the bending angle of GPS signals.

After calculating the profile of bending angles for both GPS signals (α_1, α_2), the two profiles are combined to remove the ionospheric effect from the calculated bending (Vorob'ev, 1994).

$$\alpha(a) = \frac{f_1^2 \alpha_1(a) - f_2^2 \alpha_2(a)}{f_1^2 - f_2^2} \tag{1}$$

where, a is the impact parameter, and f_i are the GPS signal frequencies. Finally, having an ionosphere free bending $\alpha(a)$, the refractive index of atmospheric can be calculated from the following relationship (Kursinski et al., 1997).

$$n(r) = exp\left[\frac{1}{\pi}\int_x^\infty \frac{\alpha}{\sqrt{a^2 - x^2}} da\right] \tag{2}$$

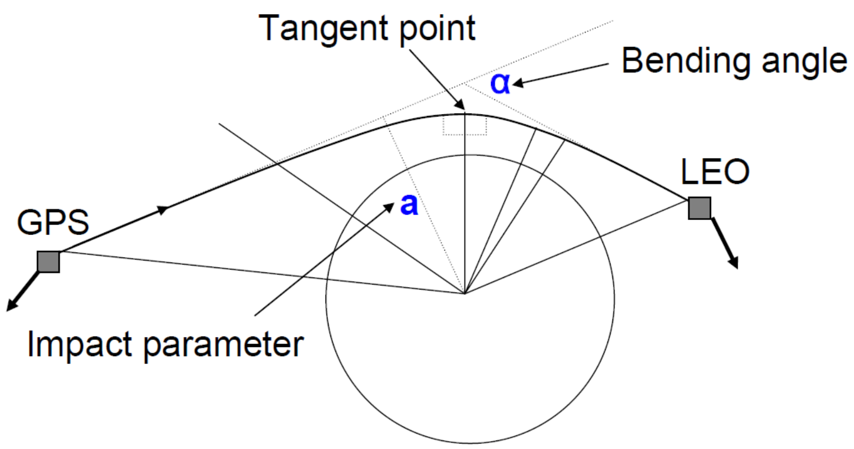

Figure 2. The geometry of a GPS RO measurement (Eyre, 2008).

In the neutral atmosphere, the refraction values (N) are related to geophysical parameters with the following equation (Hajj et al., 2002).

$$N = (n-1) \times 10^6 = a_1 \frac{P}{T} + a_2 \frac{P_w}{T^2} \qquad (3)$$

In Equation 3, the coefficients a_1 and a_2 are equal to $77.6\ ^{K}/_{mbar}$ and $3.73 \times 10^5\ ^{K^2}/_{mbar}$. To calculate the values of pressure P, temperature T and water vapor pressure P_w from the refractivity, hydrostatic equilibrium and the ideal gas law are used as additional constraints.

$$\frac{dP}{dh} = -g\rho \qquad (4)$$

$$\rho = \rho_d + \rho_w = \frac{m_d P}{TR} + \frac{(m_w - m_d)P_w}{TR} \qquad (5)$$

Where, g and h are gravity acceleration and height. Also, ρ, ρ_d and ρ_w are the total, dry air, and water vapor densities, respectively (Hajj et al., 2002). R is the universal gas constant, and m_d and m_w are the mean molecular masses of dry air and water vapor, respectively.

By combining Equations 4 and 5 and using Equation 3, the following differential equation results:

$$\frac{dP}{dh} = -\frac{gm_d}{a_1 R} N + \frac{a_2 g m_d}{a_1 R} \frac{P_w}{T^2} + \frac{g(m_w - m_d)}{R} \frac{P_w}{T} \qquad (6)$$

In areas where the water vapor pressure is negligible, one can estimate the temperature and pressure values by solving two equations with two unknowns using equations 3 and 6 together with the known N values (Hajj et al., 2002). In the tropospheric layer, where the values of water vapor pressure are significant, the estimation of all three variables of Equation 3 is carried out using variational data assimilation methods (Poli et al., 2002).

4. Results

After providing the GPS RO and radiosonde data during the study period, the RO temperature profiles were collected with distance and time differences less than 200 km and 3 h from each radiosonde data. In Fig. 3, several COSMIC temperature profiles corresponding to radiosonde observations at OIII, OIMB, OISS, OICC, and OITT stations were compared. As seen, there is a good agreement between the RO (blue dots) and radiosonde (black squares) data. The temperature profiles of these two methods were compared at different times of the year, as shown in Fig. 3. For example, the graph of the Mehrabad station (OIII) in Fig. 3 shows that the temperature profile of the GPS RO has been acquired by processing the first COSMIC satellite (C001) observations on day 341, 2010, at 22:48, along with observations of the 6th GPS (satellite G06). Moreover, the temperature profiles of the stations in Shiraz and Kermanshah were taken during the day and those of other stations at night.

As shown in Fig. 3, the high vertical resolution of GPS RO profiles demonstrates a continuous graph of temperature.

The high density of GPS RO data at different vertical levels gives more detail of the atmosphere and allows for more accurate monitoring of temperature variations in different layers. In addition, the GPS RO and radiosonde temperature profiles are consistent throughout the day and night. This is due to the high stability of GPS observations over time, and therefore, the day and night observations have equal accuracies. Hence, GPS RO data can be utilized for various climatic and meteorological applications.

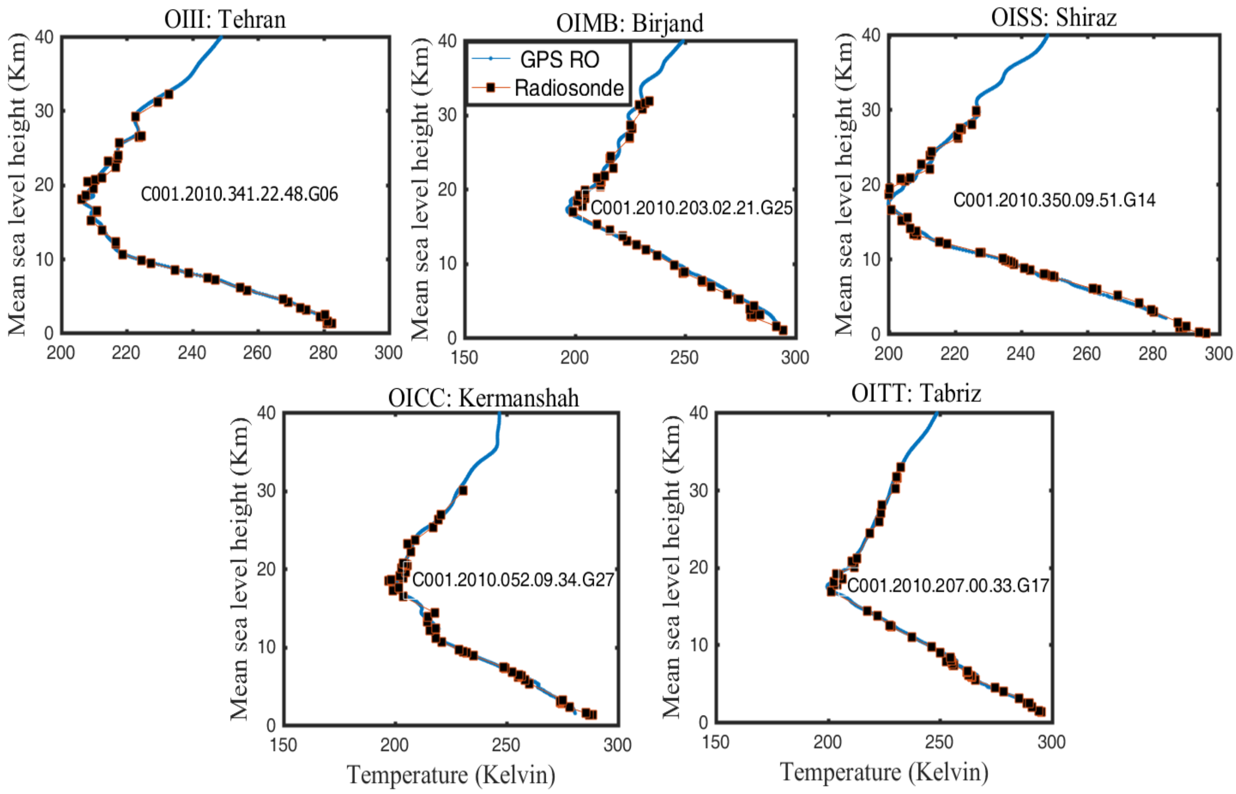

Figure 3. Comparison of GPS RO temperature profiles with radiosonde observations at the study stations in 2010

One of the objectives of this work is to investigate the accuracy of the GPS RO method at different altitudes. For this purpose, the differences between GPS RO and radiosonde temperatures were studied at 0 to 4km, 4 to 8 km, 8 to 12 km, 12 to 16 km, 16 to 20 km, 20 to 24 km, 24 to 28 km, 28 to 32 km, and 32 to 36 km. For instance, at the 8 to 12 km elevation layer, all corresponding data from both methods were extracted, and two 13-year time series were obtained at each station. Then, the temperature data of these methods were compared in terms of statistics, such as bias and standard deviation.

The mean bias and standard deviation of radiosonde - GPS RO temperature differences based on 13-year datasets gathered at five stations are given in Table 3. Based on the statistical results presented in Table 3, the mean absolute of bias values between the RO and radiosonde temperatures at altitudes below 28 km for the OIII, OIMB, OISS, OICC, and OITT stations were estimated 0.19K, 0.56, 0.16, 0.31, and 0.24 K, respectively. According to Table 3, the temperature bias values vary from 0.5 K to 1.5 K at altitudes above 28 km.

Furthermore, compared to GPS RO profiles at altitudes below 12 km, the radiosonde temperature had a negative bias at almost all of the stations. On the other hand, the mean radiosonde temperature difference from GPS RO data at altitudes above 12 km was positive for all of the stations. This result revealed the dry bias of the radiosonde temperature compared to GPS RO profiles in the upper troposphere and stratosphere of the study area.

In general, the average standard deviation values of radiosonde-GPS RO temperature differences at stations OIII, OIMB, OISS, OICC, and OITT were estimated 1.41, 1.62, 1.57, 1.47 and 1.51 K, respectively. It should be noted that the difference between radiosonde and GPS RO is not solely related to the error of retrieving RO profiles. Radiosondes suffer from bias and errors. Issues such as the incompatibility of the location of RO and radiosonde profiles, as well as the horizontal displacement between the start and end of radiosonde measurements up to 200 km, can increase the temperature differences between the two approaches. Also, the RO profile was not entirely vertical, and the position of tangent points in every single profile can vary horizontally up to 100 km (Sun et al., 2010; Norman et al., 2014).

However, the statistical outcomes obtained from the accuracy of GPS RO temperature profiles are in agreement with previous studies (Wickert et al., 2001; Hajj et al., 2004; Zhang et al., 2007; Norman et al., 2014).

Table 3. Mean and standard deviation of the differences between the radiosonde and GPS RO temperatures based on the corresponding datasets from 2006 to 2018 in five stations over Iran.

Height interval	OIII		OIMB		OISS		OICC		OITT	
	MBE	STD	MBE	STD	MBE	STD	MBE	STD	MBE	STD
0-4 km	-0.26	0.84	-0.54	1.34	-0.35	1.21	-0.52	1.35	-0.01	0.91
4-8 km	0.23	1.27	0.01	1.93	0.26	1.76	-0.15	1.24	0.04	1.30
8-12 km	-0.10	1.03	-0.30	1.30	-0.05	1.07	-0.21	1.09	-0.02	1.31
12-16 km	0.02	1.34	0.42	1.44	0.07	1.21	0.28	1.28	0.47	1.53
16-20 km	0.19	1.89	1.33	2.01	0.07	2.10	0.35	1.88	0.31	1.90
20-24 km	0.17	1.90	0.74	1.81	0.16	1.90	0.35	1.75	0.33	1.89
24-28 km	0.39	1.60	0.58	1.66	0.17	1.80	0.36	1.75	0.50	1.77
28-32 km	0.69	1.90	0.75	1.82	0.48	1.99	0.76	1.9	0.60	2.05
32-36 km	0.89	2.14	1.6	1.65	0.72	1.94	1.1	1.84	0.47	2.11

The results presented in Table 3 show the mean statistical agreement of GPS RO temperatures relative to radiosonde over 13 years. Therefore, another goal of this study is to investigate the accuracy of these data on a seasonal scale. Seasonal analysis of GPS RO temperature error statistics can help realize the performance of these data at different time scales. As a result, the Radiosonde-GPS RO temperature difference for each station and different seasons was investigated separately.

Moreover, the mean annual correlation coefficient of the radiosonde temperature and the corresponding values retrieved by GPS RO were calculated throughout the study area and are presented in Table 4. As seen, there is a high correlation of 0.99 percent between the GPS RO and radiosonde measurements for all of the years.

The mean bias and standard deviation of the Radiosonde-GPS RO temperature difference for four different seasons in the Iranian region are shown in Fig 4 and 5, respectively. According to Figure 4, seasonal comparisons at different stations emphasize that the mean bias behavior has not significantly changed from season to season. In nearly all seasons of the year, the absolute value of the bias magnitude increases slightly at higher altitudes. Generally, the bias value of the radiosonde GPS RO temperature difference (gray graphs in Fig. 4) varies from -0.5 to 0.5 K at different heights.

Considering the average standard deviation of seasonal temperature differences shown in Fig. 5, it can be seen that, except for the autumn season at OIII and OICC stations, the graphs are almost similar in various seasons.

Therefore, the accuracy of GPS RO temperature data is not significantly correlated with seasonal variations. The results also indicate that the standard deviations above 30 km of altitude increase at almost entirely stations. The standard deviation of temperature differences between these two methods in general (gray graphs in Fig. 5) was estimated to be less than 2 K.

Table 4. The annual average of correlation coefficients between radiosonde measurements and corresponding values of GPS RO temperature over the study area

Year	Mean correlation coefficient	Number of collocated profiles
2006	0.9916	1226
2007	0.9835	3401
2008	0.9905	4684
2009	0.9934	4352
2010	0.9918	4067
2011	0.9888	3913
2012	0.9832	4142
2013	0.9854	4934
2014	0.9882	4445
2015	0.9850	4697
2016	0.9904	3823
2017	0.9919	3085
2018	0.9908	1912

In addition to the seasonal examination of mean bias values, it was important to assess the accuracy of the temperature data retrieved from GPS RO over time. Time series of the annual mean bias of radiosonde-GPS RO temperature differences at nine selected altitude intervals were calculated. The results are depicted in Fig. 6.

As Fig. 6 shows, for altitudes below 28 km, the mean bias values were almost stable within a certain range over different years. Compared to another height interval, the fluctuations of mean bias values at 28-32 km (continuous dark blue line) and 32-36 km (continuous bold brown line) were higher. This might be due to the greater spatial difference between the corresponding data of the two methods at higher altitudes. In the uppermost height intervals, the analyses indicated that there was a good level of agreement between these two sets of temperature data with an average annual bias of 1.5 K.

5. Summary and conclusions

Continuous accurate and stable observations of the atmospheric structure which provide sufficient temporal and spatial resolution are of great importance in many meteorological studies and climatic analyses. Therefore, the use of new space-based methods along with conventional measuring instruments, such as radiosonde, can play a significant role in providing valuable datasets from the atmospheric structure of an area.

GPS RO, as a new method of remote sensing of the Earth's atmosphere, has played an important role in studying and monitoring various meteorological phenomena. However, due to the limited understanding of Iranian researchers and meteorologists, the long-term study and evaluation of GPS RO temperature profiles in Iran were necessary. To this end, the RO data collected from 2006 to 2018 using COSMIC, GRACE, SACC, KOMPSAT-5, KOMPSAT-5, METOP-A, and METOP-B satellite missions in Iran were compared to radiosonde data.

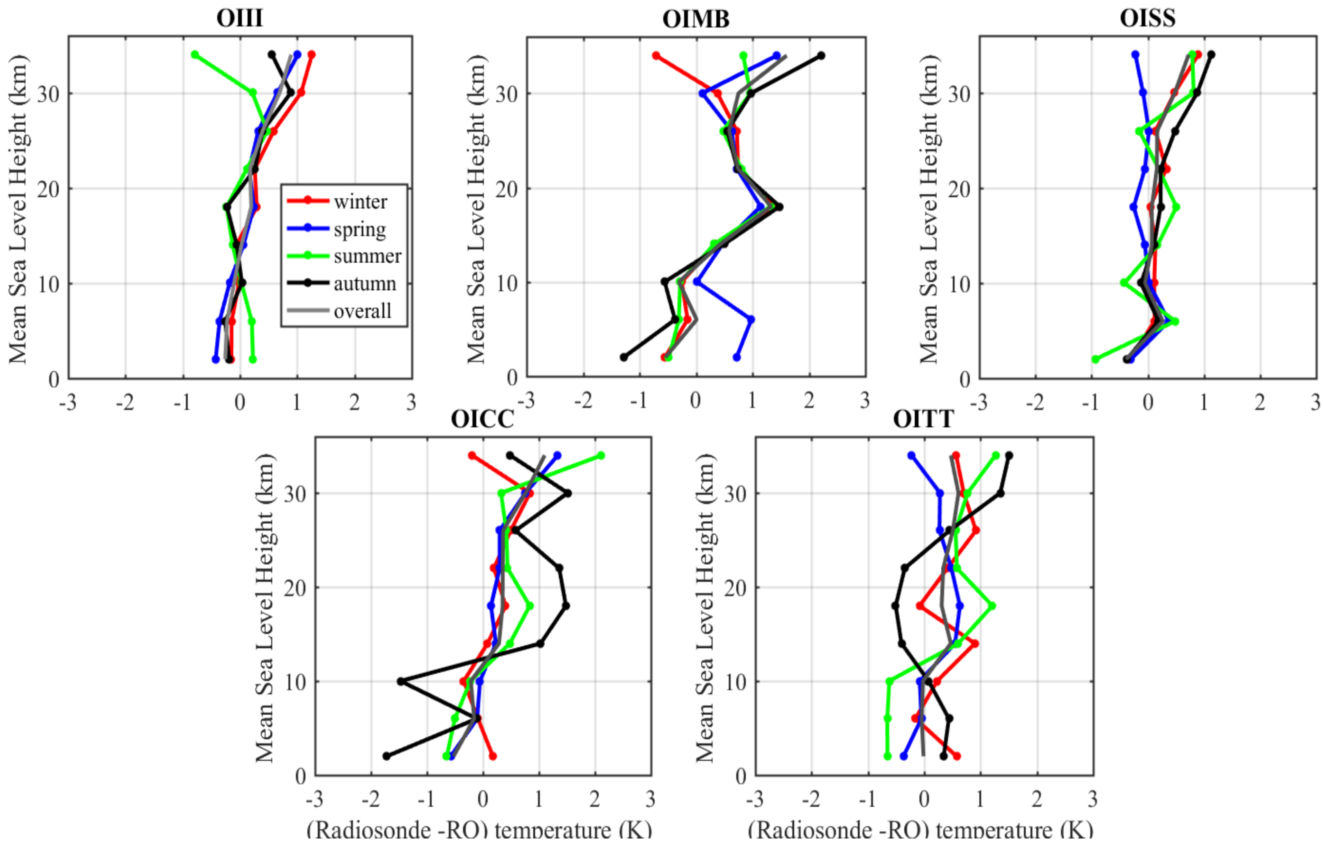

Figure 4. Average radiosonde-GPS RO temperature bias for different seasons over Iran, based on data from 2006 to 2018.

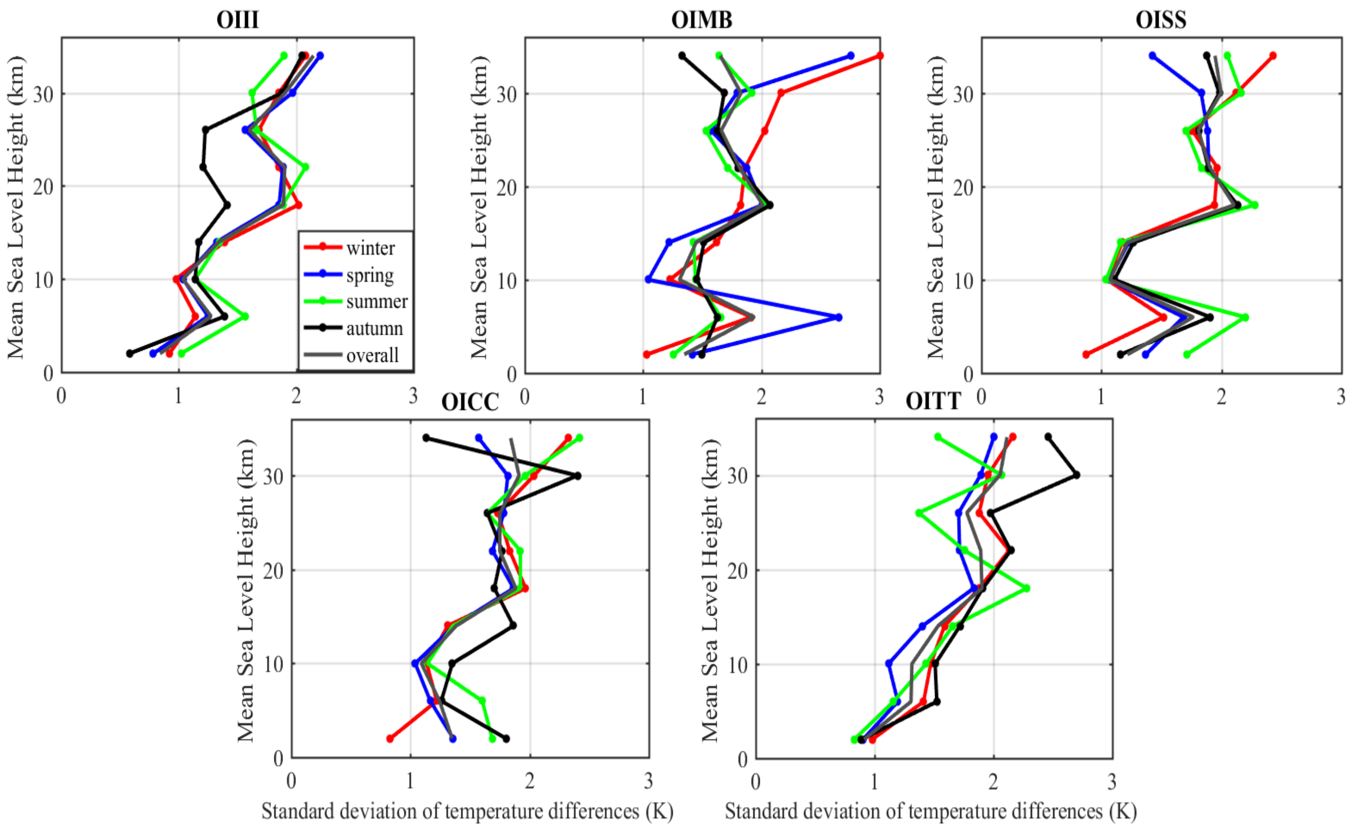

Figure 5. Average standard deviation of radiosonde-GPS RO temperature differences for distinct seasons over Iran, based on data from 2006 to 2018.

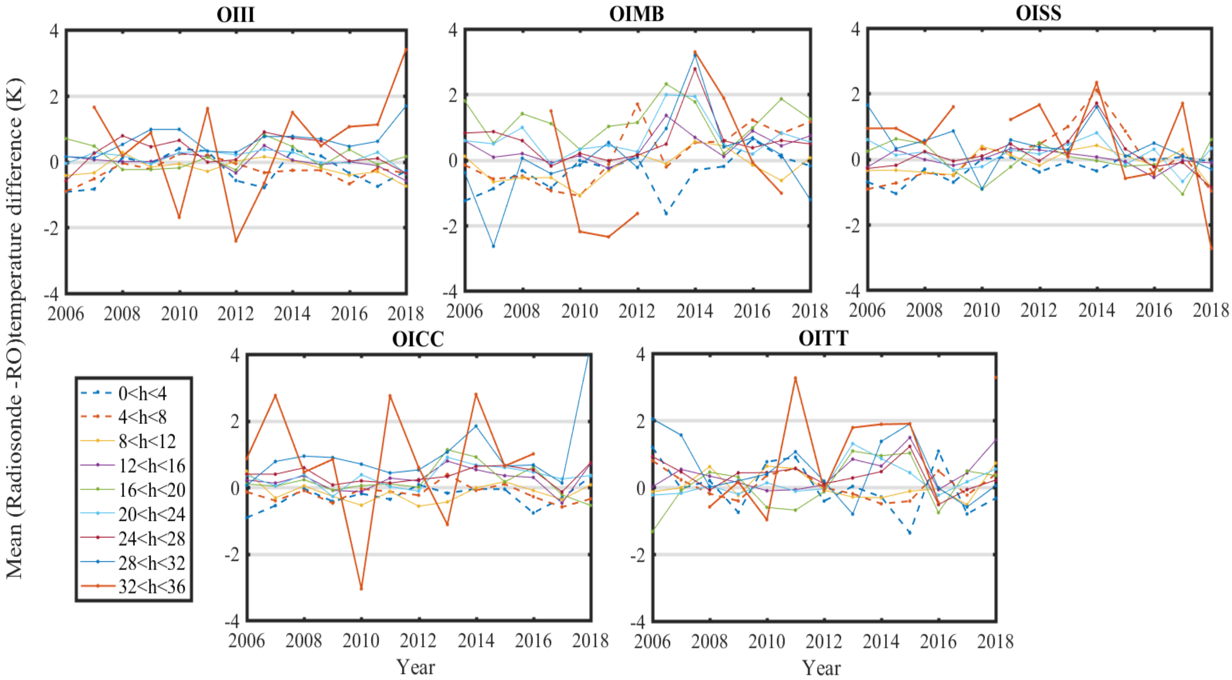

Fig. 6 Time series of mean annual bias of radiosonde –GPS RO temperature differences at OIII, OIMB, OISS, OICC, and OITT stations from 2006 to 2018.

In order to evaluate the RO temperature data more accurately, error statistics were calculated at geographically different stations and nine various altitude intervals.

Statistical comparison of GPS RO data with those of the radiosonde at five stations in regions with different climates confirmed a high agreement between the two methods. Based on the data of 13 years, the average bias temperature of the GPS RO relative to the radiosonde was estimated to be less than 0.5 K at altitudes below 28 km. The results also indicated that the radiosonde underestimates temperature compared to the GPS RO below 12 km, with a dry bias above this altitude.

Based on the time series of temperature differences at all stations and altitude layers, the average standard deviation was estimated to be about 1.5 K, which is in agreement with previous works. Also, the seasonal behavior of error statistics for GPS RO temperatures was examined in the study area. In general, the behavior of bias graphs and the standard deviation of radiosonde-GPS RO temperature difference in the region did not show any significant dependence on seasonal variations. For almost all seasons and stations, the bias and standard deviation values increased for altitudes above 30 km.

As a final point, in order to understand the stability of the accuracy of GPS RO temperatures, the time series of the annual mean bias at all stations were investigated. According to the results, for most of the altitude intervals, the bias values did not vary highly in different years. These findings indicate the stability of GPS RO temperature profiles in the study area. The results of this research can provide useful information about the potential and efficiency of GPS RO techniques to the users in the study region. Thus, they can utilize these valuable temperature data more confidently.

Acknowledgment

The author would like to thank the reviewers and editors for their thoughtful and constructive comments and suggestions and acknowledges the funding support of the Babol Noshirvani University of Technology for Grant program No. BNUT/394099/97.

References

Anthes, R. A., Rocken, C., & Ying-Hwa, K. (2000). Applications of COSMIC to meteorology and climate. *Terrestrial, Atmospheric and Oceanic Sciences*, 11(1), 115-156.

Anthes, R. A., Bernhardt, P. A., Chen, Y., Cucurull, L., Dymond, K. F., Ector, D., ... & Liu, H. (2008). The COSMIC/FORMOSAT-3 mission: Early results. *Bulletin of the American Meteorological Society*, 89(3), 313-334.

Aparicio, J. M., & Deblonde, G. (2008). Impact of the assimilation of CHAMP refractivity profiles on Environment Canada global forecasts. *Monthly weather review*, 136(1), 257-275.

Bird, M. K., Asmar, S. W., Brenkle, J. P., Edenhofer, P., Funke, O., Pätzold, M., & Volland, H. (1992). Ulysses radio occultation observations of the lo plasma torus during the Jupiter encounter. Science, 257(5076), 1531-1535.

Bohlinger, P., Sinnhuber, B. M., Ruhnke, R., & Kirner, O. (2014). Radiative and dynamical contributions to past and future Arctic stratospheric temperature trends. *Atmospheric Chemistry & Physics Discussions*, 14(3).

Chang, L., Guo, L., Feng, G., Wu, X., Gao, G., Zhang, Y., & Zhang, Y. (2018). Comparison of the Arctic upper-air temperatures from radiosonde and radio occultation observations. *Acta Oceanologica Sinica*, 37(1), 30-39.

Divakarla, M. G., Barnet, C. D., Goldberg, M. D., McMillin, L. M., Maddy, E., Wolf, W., ... & Liu, X. (2006). Validation of Atmospheric Infrared Sounder temperature and water vapor retrievals with matched radiosonde measurements and forecasts. *Journal of Geophysical Research: Atmospheres*, 111(D9).

Eyre, J. R. (2008, June). An introduction to GPS radio occultation and its use in numerical weather prediction. *In Proceedings of the ECMWF GRAS SAF Workshop on Applications of GPS Radio Occultation Measurements* (Vol. 1618).

Foelsche, U., Pirscher, B., Borsche, M., Kirchengast, G., & Wickert, J. (2009). Assessing the climate monitoring utility of radio occultation data: From CHAMP to FORMOSAT-3/COSMIC. *Terrestrial, Atmospheric & Oceanic Sciences*, 20(1).

Hajj, G. A., Ibanez‐ Meier, R., Kursinski, E. R., & Romans, L. J. (1994). Imaging the ionosphere with the Global Positioning System. *International Journal of imaging systems and Technology*, 5:174–184.

Hajj, G. A., Kursinski, E. R., Romans, L. J., Bertiger, W. I., & Leroy, S. S. (2002). A technical description of atmospheric sounding by GPS occultation. *Journal of Atmospheric and Solar-Terrestrial Physics*, 64(4), 451-469.

Hajj, G. A., Ao, C. O., Iijima, B. A., Kuang, D., Kursinski, E. R., Mannucci, A. J., ... & Yunck, T. P. (2004). CHAMP and SAC‐ C atmospheric occultation results and intercomparisons. *Journal of Geophysical Research*, 109(D6).

Healy, S. B., Jupp, A. M., & Marquardt, C. (2005). Forecast impact experiment with GPS radio occultation measurements. *Geophysical Research Letters*, 32(3).

Ho, S. P., Hunt, D., Steiner, A. K., Mannucci, A. J., Kirchengast, G., Gleisner, H., ... & Schreiner, W. (2012). Reproducibility of GPS radio occultation data for climate monitoring: Profile‐ to‐ profile inter‐ comparison of CHAMP climate records 2002 to 2008 from six data centers. *Journal of Geophysical Research*, 117(D18).

Ho, S. P., Peng, L., & Vömel, H. (2017). Characterization of the long-term radiosonde temperature biases in the upper troposphere and lower stratosphere using COSMIC and Metop-A/GRAS data from 2006 to 2014. Atmos. Chem. Phys, 17, 4493-4511.

Sam Khaniani, A., & Ghahremani, M. (2019). Estimation of GPS Tropospheric delays using different data processing strategies in Iran. *Annals of Geophysics*, 61(6), 663.

Sam Khaniani, A., Nikraftar, Z., & Zakeri, S. (2020). Evaluation of MODIS Near-IR water vapor product over Iran using ground-based GPS measurements. *Atmospheric Research*, 231, 104657.

Kishore, P., Namboothiri, S. P., Jiang, J. H., Sivakumar, S., & Igarashi, K. (2009). Global temperature estimates in the troposphere and stratosphere: a validation study of COSMIC/FORMOSAT-3 measurements. Atmos. Chem. Phys., 9, 897–908, 2009

Kuo, Y. H., Schreiner, W. S., Wang, J., Rossiter, D. L., & Zhang, Y. (2005). Comparison of GPS radio occultation soundings with radiosondes. *Geophysical Research Letters*, 32(5).

Kursinski, E. R., Hajj, G. A., Bertiger, W. I., Leroy, S. S., Meehan, T. K., Romans, L. J., ... & Yunck, T. P. (1996). Initial results of radio occultation observations of Earth's atmosphere using the Global Positioning System. Science, 271(5252), 1107-1110.

Kursinski, E. R., Hajj, G. A., Schofield, J. T., Linfield, R. P., & Hardy, K. R. (1997). Observing Earth's atmosphere with radio occultation measurements using the Global Positioning System. *Journal of Geophysical Research*, 102(D19), 23429-23465.

Le Marshall, J., Xiao, Y., Norman, R., Zhang, K., Rea, A., Cucurull, L., ... & Le, T. (2010). The beneficial impact of radio occultation observations on Australian region forecasts. Aust. Meteorol. Oceanogr. J, 60, 121-125.

Le Marshall, J., Xiao, Y., Norman, R., Zhang, K., Rea, A., Cucurull, L., ... & Le, T. (2012). The application of radio occultation observations for climate monitoring and numerical weather prediction in the Australian Region. Aust Meteorol Oceanogr J, 62, 323-334.

Luers, J. K. (1997). Temperature error of the Vaisala RS90 radiosonde. *Journal of Atmospheric and Oceanic Technology*, 14, 1520–1532.

Norman, R., Le Marshall, J., Zhang, K., Wang, C. S., Carter, B. A., Rohm, W., ... & Li, Y. (2014). Comparing GPS Radio Occultation Observations with Radiosonde Measurements in the Australian Region. *In Earth on the Edge: Science for a Sustainable Planet* (pp. 51-57). Springer, Berlin, Heidelberg.

Phinney, R. A., & Anderson, D. L. (1968). On the radio occultation method for studying planetary atmospheres. J *Journal of Geophysical Research*, 73(5), 1819-1827.

Poli, P., Joiner, J., & Kursinski, E. R. (2002). 1DVAR analysis of temperature and humidity using GPS radio occultation refractivity data. *Journal of Geophysical Research*, 107(D20), ACL-14.

Reigber, C., Schwintzer, P., Lühr, H., and Wickert, J. (2005) Earth Observation with CHAMP : Results from Three Years in Orbit. 628 p. Springer, Berlin.

Rennie, M. P. (2010). The impact of GPS radio occultation assimilation at the Met Office. *Quarterly Journal of the Royal Meteorological Society: A journal of the atmospheric sciences, applied meteorology and physical oceanography*, 136(646), 116-131.

Rocken, C., Anthes, R., Exner, M., Hunt, D., Sokolovskiy, S., Ware, R., ... & Kuo, Y. H. (1997). Analysis and validation of GPS/MET data in the neutral atmosphere. *Journal of Geophysical Research*, 102(D25), 29849-29866.

Rossiter, D. (2003). Comparison Between GPS Radio Occultation and Radiosonde Sounding Data.

Seidel, D. J., Gillett, N. P., Lanzante, J. R., Shine, K. P., & Thorne, P. W. (2011). Stratospheric temperature trends: Our evolving understanding. *Wiley Interdisciplinary Reviews: Climate Change*, 2(4), 592-616.

Sharifi, M. A., Khaniani, A. S., Masoumi, S., Schmidt, T., & Wickert, J. (2013a). Least-squares harmonic estimation of the tropopause parameters using GPS radio occultation measureents. *Meteorology and Atmospheric Physics*, 120(1-2), 73-82.

Sharifi, M. A., Sam-Khaniani, A., Joghataei, M., Schmidt, T., Masoumi, S., & Wickert, J. (2013b). Tropopause analysis over the Iranian region using GPS radio occultation data. Advances in Space Research, 52(9), 1700-1707.

Mohammad Ali Sharifi, Majid Azadi, Ali Sam-Khaniani, (2016), Numerical simulation of rainfall with assimilation of conventional and GPS observations over north of Iran. *Annals of Geophysics*, *59*(3), 0322.

Sobrino, J. A., Jiménez-Muñoz, J. C., Mattar, C., & Sòria, G. (2015). Evaluation of Terra/MODIS atmospheric profiles product (MOD07) over the Iberian Peninsula: A comparison with radiosonde stations. *International Journal of Digital Earth*, 8(10), 771-783.

Sun, B., Reale, A., Seidel, D. J., & Hunt, D. C. (2010). Comparing radiosonde and COSMIC atmospheric profile data to quantify differences among radiosonde types and the effects of imperfect collocation on comparison statistics. *Journal of Geophysical Research*, 115, D23104.

Thorne, P. W., Brohan, P., Titchner, H. A., McCarthy, M. P., Sherwood, S. C., Peterson, T. C., ... & Fereday, D. R. (2011). A quantification of uncertainties in historical tropical tropospheric temperature trends from radiosondes. *Journal of Geophysical Research*, 116(D12).

Tsuda, T., & Hocke, K. (2004). Application of GPS radio occultation data for studies of atmospheric waves in the middle atmosphere and ionosphere. *Journal of the Meteorological Society of Japan. Ser*. II, 82(1B), 419-426.

UCAR. (2006) New Satellite System will Use GPS Signals to Track Hurricanes, Climate Chang, and Space Weather. Innovative U.S.-Taiwan Satellite Constellation To Be Launched Friday. The National Center for Atmospheric Research & the UCAR Office of Program, http://www.ucar.edu/news/releases/2006/cosmic.shtml.

Vorob'ev, V. V. (1994). Estimation of the accuracy of the atmospheric refractive index recovery from Doppler shift measurements at frequencies used in the NAVSTAR system. *Atmospheric and Oceanic Physics*, 29, 602-609.

Ware, R., Exner, M., Feng, D., Gorbunov, M., Hardy, K., Herman, B., ... & Schreiner, W. (1996). GPS sounding of the atmosphere from low Earth orbit: Preliminary results. *Bulletin of the American Meteorological Society*, 77(1), 19-40.

Wickert, J., Reigber, C., Beyerle, G., König, R., Marquardt, C., Schmidt, T., ... & Hocke, K. (2001). Atmosphere sounding by GPS radio occultation: First results from CHAMP. *Geophysical research letters*, 28(17), 3263-3266.

Wickert, J., Schmidt, T., Beyerle, G., König, R., Reigber, C., & Jakowski, N. (2004). The radio occultation experiment aboard CHAMP: Operational data analysis and validation of vertical atmospheric profiles. *Journal of the Meteorological Society of Japan.* II, 82(1B), 381-395.

Zhang, K., Biadeglgne, B., Wu, F., Kuleshov, Y., Rea, A., Hodet, G., & Fu, E. (2007). A comparison of atmospheric temperature and moisture profiles derived from GPS radio occultation and radiosone in Australia. *In Workshop for Space, Aeronautical and Navigational Electronics, Perth, Australia, April* (Vol. 12).